



Cite this: DOI: 10.1039/c5nj01981h

Facile synthesis of a biocompatible silver nanoparticle derived tripeptide supramolecular hydrogel for antibacterial wound dressings†

Turibius Simon, Chung-Shu Wu, Jie-Chuan Liang, Chieh Cheng and Fu-Hsiang Ko*

Realizing the widespread demand for biocompatible supramolecular hydrogel based wound dressings, we have developed an N-terminally 2(naphthalen-6-yl)acetic acid (Nap) protected Phe–Phe–Cys peptide (Nap-FFC) using a liquid phase method. This Nap-FFC peptide was used to design a supramolecular hydrogel via a self-assembling process. The Nap-FFC short peptides produced stable and transparent silver nanoparticle-based hydrogels (AgNPs@Nap-FFC) wherein the self-assembled Nap-FFC nanofibers acted as scaffolds for the mineralization of silver nanoparticles (AgNPs) and stabilizers of the synthesized AgNPs. The resultant AgNPs@Nap-FFC nanocomposites were characterized using ultraviolet-visible spectrophotometry (UV-vis spectroscopy), Fourier transform infrared spectroscopy (FT-IR), transmission electron microscopy (TEM) and scanning electron microscopy (SEM) combined with energy-dispersive X-ray spectroscopy (EDX) studies. The AgNPs@Nap-FFC nanocomposites showed excellent monodispersity, long term stability, and functional flexibility in comparison to other AgNP based nanocomposites. Furthermore, AgNPs@Nap-FFC exhibited strong inhibition against both Gram-positive (methicillin-resistant *Staphylococcus aureus*) and Gram-negative (*Acinetobacter baumannii*) bacteria and, most importantly, they showed favorable biocompatibility towards human cervical carcinoma cells (HeLa cells). Hence, this study implies that AgNPs@Nap-FFC nanocomposites can easily be prepared in a cost-effective manner and can be used effectively for future antibacterial wound dressings.

Received (in Montpellier, France)
30th July 2015,

Accepted 8th December 2015

DOI: 10.1039/c5nj01981h

www.rsc.org/njc

Introduction

Much attention has been devoted to the pharmacology of silver nanoparticles (AgNPs) in terms of their large surface area to volume ratio, physicochemical properties, antioxidant activity and low toxicity to mammalian cells.^{1–3} AgNPs induce the production of hydroxyl radicals ($\bullet\text{OH}$) to kill bacterial cells, without interacting with the multidrug-resistant pumps in bacteria that produce toxins to inhibit antibiotics like ampicillin. This suggests that resistance to AgNPs is less likely to occur in bacteria and hence it can be used as a new generation antimicrobial agent to overcome the drug resistance seen with Gram-negative and Gram-positive bacteria.^{4,5} This unique character enabled AgNPs to be used in a wide variety of products such as refrigerators, clothes, toothbrushes, and cosmetics.⁶ AgNPs have been shown to have superior cytotoxicity against a wide range of microorganisms when compared to many metal nanoparticles.⁷ However, bare AgNPs (e.g. sodium borohydride/citrate reduced AgNPs) are unstable

in aqueous medium, due to the release of surface bound Ag^+ ions thereby, causing the loss of antibacterial activity and inducing cellular toxicity and reactive oxygen species (ROS) production to normal cells upon overtime exposure.^{8,9} Hence there is a need to synthesize stable biocompatible AgNPs in order to reduce their cellular toxicity in health care or biomedical applications.^{10,11} Different polymer nanocomposites such as poly(oxyethylene)-segmented imide (POEM), poly(styrene-co-maleic anhydride)-grafting poly(oxyalkylene) (SMA) and poly(vinyl alcohol) (PVA) have been employed to stabilize AgNPs and been used for biomedical applications.¹² But the stabilization of polymer based nanocomposite materials requires prolonged synthesis steps and high cost, and shows inadequate biocompatibility.¹³

To improve the biocompatibility and to shorten the synthesis steps, proteins or artificial self-assembling peptide-based scaffolds are employed to synthesise peptide based nanocomposite materials through a biomineralization mechanism.¹⁴ Common biomimetic peptides include the fibronectin-derived RGDS sequence for therapeutic cell delivery,¹⁵ the laminin derived IKVAV sequence¹⁶ used for bone regeneration and wound healing, etc. In addition, self-assembled peptide-based hydrogels could be used for various therapeutic approaches such as the regeneration of enamel, cartilage, and the central nervous system, as well as

Department of Materials Science and Engineering, National Chiao Tung University, 1001 University Road, Hsinchu, Taiwan 300, Republic of China.

E-mail: fhko@mail.nctu.edu.tw; Tel: +886-35712121 ext 55803

† Electronic supplementary information (ESI) available. See DOI: 10.1039/c5nj01981h

delivery vehicles, transplantation of islets, wound-healing and cardiovascular therapies.^{17,18} Among the self-assembling peptides used,¹⁹ the diphenylalanine (FF) peptide and its derivatives can be more easily self-assembled into various nanostructures than other lengthy peptides applied for biomedical applications.²⁰ Proceeding from these research reports, we decided to introduce an efficient peptide-tunable hydrogel, co-fabricated with AgNPs. Accordingly, an N-terminally protected FF peptide derivative (Nap-FFC) was synthesized in laboratory-scale, which showed a robust metal binding ability with AgNPs and was able to form stable and transparent AgNPs@Nap-FFC hydrogels. The synthetic reactions were mild and environment friendly. Furthermore, bioassays revealed that the synthesized AgNPs@Nap-FFC nanocomposites possess an effective and long term antibacterial activity against both Gram-positive bacteria and Gram-negative bacteria. Most importantly, the AgNPs@Nap-FFC hydrogels were proven to be non-toxic to human cells, and therefore this approach would be a versatile platform in mechanobiology. Due to the strong bacterial inhibition activity, this novel AgNPs@Nap-FFC hydrogels could be an attractive antibacterial material for use as wound dressings in biomedical applications.

Materials and methods

Chemicals and reagents

2(Naphthalen-6-yl)acetic acid (Nap), *N,N'*-dicyclohexylcarbodiimide (DCC), *N*-hydroxysuccinimide (NHS), *L*-phenylalanine (Phe), *L*-cysteine (Cys) and sodium carbonate (Na₂CO₃) were purchased from Alfa Aesar and used without further purification. Silver nitrate (AgNO₃), sodium borohydride (NaBH₄), chloroform (CHCl₃) and methanol (CH₃OH) were obtained from Aldrich, U.S.A. Metal salts such as ZnCl₂, MgCl₂, AgCl₂, FeCl₂, CoCl₂, CdCl₂, BaCl₂, LiCl, NiCl₂, KCl and CaCl₂ were from Baker Analyzed ACS Reagent, U.S.A. Bacterial strains (methicillin-resistant *Staphylococcus aureus* and *Acinetobacter baumannii*) and HeLa cell lines were from the BCRC (Bioresource Collection and Research Center) Taiwan. Bacterial culture media such as trypticase soy broth (TSB) and trypticase soy agar (TSA) were purchased from Becton, Dickinson and Company. The medium used for the culture of HeLa cells was Dulbecco's modified eagle medium (DMEM-Thermo Scientific).

Instruments and product characterization

The molecular structures of Nap-F, Nap-FF, and Nap-FFC were elucidated *via* nuclear magnetic resonance spectroscopy (NMR, Bruker 300 MHz spectrometer) and high resolution mass analysis (HRMS, Waters Premier XE instrument with ESI source). The ionic interactions of Nap-FFC with various metal ions were determined using Fourier transform infrared spectroscopy (FTIR, Perkin Elmer spectrometer 100 FT-IR SPECTRUM ONE) and compared deduced reactions. The silver nanoparticles (AgNPs) and silver based Nap-FFC nanocomposites (AgNPs@Nap-FFC) were characterized *via* UV-vis spectroscopy (HITACHI, U-3310), scanning electron microscopy (SEM, JEOL, JSM-6700) and transmission electron microscopy (TEM, JEOL, JEM-2100).

Synthesis of a biocompatible peptide

N-terminally Nap protected peptide Nap-FFC (Nap-Phe-Phe-Cys) was synthesized using a liquid phase method.²¹

Synthesis of Nap-F

2(Naphthalen-6-yl)acetic acid (Nap, 372 mg, 2 mmol) and *N*-hydroxysuccinimide (NHS, 230 mg, 2 mmol) were dissolved in 20 mL chloroform and *N,N'*-dicyclohexylcarbodiimide (DCC, 432 mg, 2.1 mmol) was added. The mixture was stirred at room temperature for 5 h, then the resulting solid was filtered off, and the filtrate was subjected to rotary evaporation. The crude product obtained (Nap-NHS) was used without purification. *L*-Phenylalanine (330 mg, 2 mmol) and sodium carbonate (Na₂CO₃, 424 mg, 4 mmol) were dissolved in 8 mL of water, the solution of the crude product (Nap-NHS) (dissolved in 20 mL acetone) was added, and the resulting reaction mixture was stirred at room temperature overnight. The reaction mixture was subjected to rotary evaporation, and then 20 mL of water was added. The filtrate was acidified to pH 3 and the resulting product obtained by filtration was further purified using a flash column with chloroform-methanol as the eluent. Compound Nap-F (white powder) was collected with 58% yield. ¹H NMR (300 MHz, DMSO-*d*₆) δ (ppm): 8.44 (d, *J* = 8.1 Hz, 1NH), 7.86–7.75 (m, 3H), 7.64 (s, 1H), 7.46 (t, *J* = 6 Hz, 2H), 7.27–7.18 (m, 6H), 4.42 (t, *J* = 4.2 Hz, 1H), 3.57 (d, 2H), 3.09–2.82 (m, 2H). HRMS (ESI⁻): calculated for C₂₁H₁₉NO₃ 333.1365 found [M – H]⁻ 332.1281.

Synthesis of Nap-FF

Compound Nap-F (333 mg, 1 mmol) and NHS (115 mg, 1 mmol) were dissolved in chloroform (10 mL) and DCC (216 mg, 1.05 mmol) was added. The mixture was stirred at room temperature for 5 h, then the resulting solid was filtered off, and the filtrate was subjected to rotary evaporation. The crude product obtained (Nap-F-NHS) was used without purification. *L*-Phenylalanine (165 mg, 1 mmol) and Na₂CO₃ (212 mg, 2 mmol) were dissolved in 4 mL of water, the solution of crude product (Nap-F-NHS) was dissolved in 10 mL of acetone, and then the resulting reaction mixture was stirred at room temperature overnight. The reaction mixture was subjected to rotary evaporation, and then 10 mL of water was added. The filtrate was acidified to pH 3, and the resulting product obtained by filtration was further purified using a flash column with chloroform-methanol as the eluent. The dipeptide Nap-FF (white powder) was collected with 50% yield. ¹H NMR (300 MHz, DMSO-*d*₆) δ (ppm): 8.29–8.49 (m, 3H), 7.42–7.86 (m, 3H), 7.10–7.28 (m, 8H), 4.44–4.59 (m, 2H, –CH), 2.95–3.10 (m, 3H), 2.68–2.92 (m, 3H). HRMS (ESI⁻): calculated for C₃₀H₂₈N₂O₄ 480.2049 found [M – H]⁻ 479.1966.

Synthesis of Nap-FFC

Compound Nap-FF (240 mg, 0.5 mmol) and NHS (57.5 mg, 0.5 mmol) were dissolved in chloroform (6 mL) and DCC (107 mg, 0.52 mmol) was added. The mixture was stirred at room temperature for 5 h, then the resulting solid was filtered off, and the filtrate was subjected to rotary evaporation. The crude product obtained (Nap-FF-NHS) was used without purification.

L-Cysteine (60.5 mg, 0.5 mmol) and Na₂CO₃ (106 mg, 1 mmol) were dissolved in 2 mL of water; the solution of crude product (Nap-FF-NHS) dissolved in 6 mL of acetone was added. And the resulting reaction mixture was stirred at room temperature overnight. The reaction mixture was subjected to rotary evaporation, and then 10 mL of water was added. The filtrate was acidified to pH 3 and the resulting product obtained by filtration was further purified using a flash column with chloroform–methanol as the eluent. The final compound Nap-FFC (white powder) was collected with 30% yield. The ¹H NMR (300 MHz, DMSO-d₆) δ (ppm): 12.93 [s (br), 1H (–COOH)], 8.25–8.48 [m, 6H (–NH & aromatic)], 7.30–7.48 [m, 3H, (aromatic)], 7.10–7.24 [m, 8H (aromatic)], 4.44–4.59 [m, 3H (–CH)], 2.95–3.09 [m, 4H (–CH₂)], 2.50–2.84 [m, 4H (–CH₂)], 1.761 [s (br), 1H (SH)]. HRMS (ESI[–]): calculated for C₃₃H₃₃N₃O₅S 583.2141 found [M – H][–] 582.2070.

Gelation properties of Nap-FFC

Different concentrations of Nap-FFC (w/v) in aqueous solution under different pH conditions were evaluated for their gelation properties.

Synthesis of silver nanoparticles (AgNPs)

62.5 μL of 0.1 M silver nitrate (AgNO₃) and freshly prepared ice cold 300 μL of 5 mM sodium borohydride (NaBH₄) were added in 25 mL of distilled water with continuous stirring. The reaction was carried out at room temperature for 30 minutes. The reaction mixture slowly turned to a yellow coloured solution, indicating the formation of AgNPs.²² The prepared AgNP solution was stored at 4 °C for further study.

Synthesis of AgNPs@Nap-FFC nanocomposites

62.5 μL of 0.1 M silver nitrate (AgNO₃) was added to 25 mL of a 120 μM Nap-FFC solution (pH 12). The mixture was gently stirred for 30 minutes at room temperature. Then, freshly prepared cold 300 μL of 5 mM sodium borohydride (NaBH₄) was added to the reaction mixture. The reaction mixture then slowly turned to a brown colour solution, indicating the formation of silver nanoparticle based Nap-FFC nanocomposites (AgNPs@Nap-FFC).

Antibacterial activity determination

The antibacterial activity of the AgNPs@Nap-FFC hydrogel was evaluated *via* direct contact with Gram positive and Gram negative bacteria. Common drug resistant bacterial strains such as methicillin-resistant *Staphylococcus aureus* and *Acinetobacter baumannii* were tested. In brief, bacterial strains cultured in 2 mL of trypticase soy broth (TSB) were treated with the AgNPs@Nap-FFC hydrogel at concentrations of 40 and 80 μg mL^{–1} of bacterial medium. Bacterial growth rates were determined by measuring the optical density (OD) at 600 nm using a spectrophotometer (cell density meter). For the bactericidal activity assay, the bacteria were grown on TSA plates at 37 °C for 24 hours to obtain the late-log growth phase (OD₆₀₀ = 2.0). The plates were incubated with a 1% (w/v) Nap-FFC hydrogel pad and AgNPs@Nap-FFC nanocomposites (80 μg mL^{–1}). Meanwhile, the 1% Nap-FFC (w/v) hydrogel pad incubated under the same environments was used as a control. The agar plates were incubated

at room temperature and the bacterial growth rates were determined by measuring the OD at 600 nm.

Biocompatibility studies using an MTT assay

In order to evaluate the cytotoxic activity of AgNPs@Nap-FFC nanocomposites, human cervical carcinoma (HeLa) cells were used in this study. HeLa cells were maintained in Dulbecco's modified Eagle's medium (DMEM) supplemented with 10% fetal bovine serum (FBS) and 1× antibiotics solution, and cultured at 37 °C in a humidified incubator containing 5% CO₂. For the cytotoxicity assay, cells were grown in 96-well plates (flat bottom) at a density of 1.5 × 10⁴ cells per well with 100 μL of the medium. After overnight culturing, the culture medium was aspirated and fresh media containing the AgNPs@Nap-FFC nanocomposites at concentrations ranging from 10 to 100 μg mL^{–1} were added and incubated for 24 h. In order to determine the viability of the HeLa cells, 100 μL of the MTT solution (5 mg mL^{–1}) diluted in serum free DMEM medium was added, and incubated at 37 °C for 4 h. After 4 h of incubation, purple colored crystals formed and were dissolved in DMSO and the absorbance was measured at 570 nm using a Multiskan GO micoplate reader. All experiments were independently performed at least three times. The results were presented as percentage of viable cells against the increasing dose of the AgNPs@Nap-FFC nanocomposites. The untreated cells served as control.

Results and discussion

Physicochemical characterization of the Nap-FFC peptide

The preparation method of the Nap protected FFC peptide (Nap-Phe-Phe-Cys) *via* liquid phase approach is illustrated in Fig. S1 (ESI[†]). The primary molecular structure of Nap-F, Nap-FF, and Nap-FFC were confirmed using the NMR spectra of each compound (Fig. S2–S4, ESI[†]). The molecular structures of the synthesized peptides, Nap-F, Nap-FF, and Nap-FFC, were further verified *via* high resolution mass analysis (Fig. S5–S7, ESI[†]). The data obtained from the NMR and high resolution mass spectra revealed the exact peptide sequence identity peak and mass value of those compounds. The supramolecular Nap-FFC peptide structure showed two different moieties: hydrophobic and hydrophilic. The hydrophobic group promotes the self-assembly process to form hydrogels. On the other hand, the hydrophilic moiety exhibits many carboxylic acid and thiol groups on the supramolecule nanofiber (Nap-FFC) surface, which can act as silver metal ion binding sites and nucleation sites for the growth of silver nanoparticles. The synthesized Nap-FFC peptide has free carboxylic acid and thiol groups which enable the tuning of the peptide nature based on the desired conditions. These peptides can self-assemble to form supramolecular hydrogels with respect to different conditions, such as the peptide weight percentage concentration (w/v), pH conditions and mineralisation with metal ions. For this study, we have taken the Nap moiety as a protecting group since it is present in clinically approved drug molecules such as propranolol and naphazoline, and are more biocompatible than the Fmoc or pyrene groups.²³ The hydrophilic moiety of

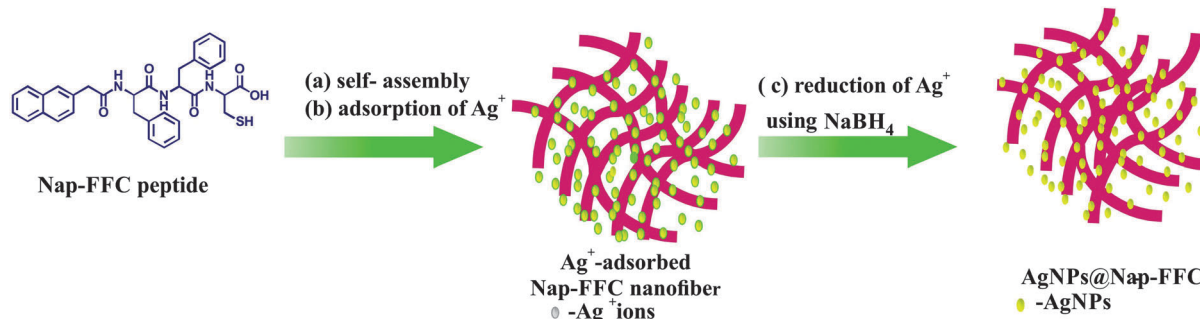


Fig. 1 Schematic illustration for the preparation process of the AgNPs@Nap-FFC nanocomposites.

Nap-FFC has numerous carboxylic acid and thiol groups on the peptide nanofiber surface, which act as nucleation sites for the growth of nanoparticles and as metal binding sites. The mineralization process of silver ions using the peptide nanofibers are shown in Fig. 1. We proposed the synthetic method of supramolecular AgNP entrapped hydrogel (AgNPs@Nap-FFC) nanocomposites. The above mechanism displays more advantages than other methods due to the ease of fabrication, good biocompatibility, cost effectiveness, the acceleration of the wound healing process, molecular recognition capability and functional flexibility.^{2,24} Metal ions can coordinate with negatively charged carboxylic acid groups and thiol groups through an electrostatic interaction process and are reduced to metal atoms. The Ag ions were able to coordinate more effectively with Nap-FFC and henceforth we used sodium borohydride which subsequently initiated the generation of Ag nuclei that finally grow into AgNPs along with peptide nanofibers. This mechanism of biomineralisation enabled the preparation of the silver nanoparticle based Nap-FFC nanocomposites (AgNPs@Nap-FFC).

Gelation property of Nap-FFC

Different pH induced phase transitions of 1% Nap-FFC hydrogel (w/v) at 30 °C are shown in Fig. 2. The 1% w/v Nap-FFC was

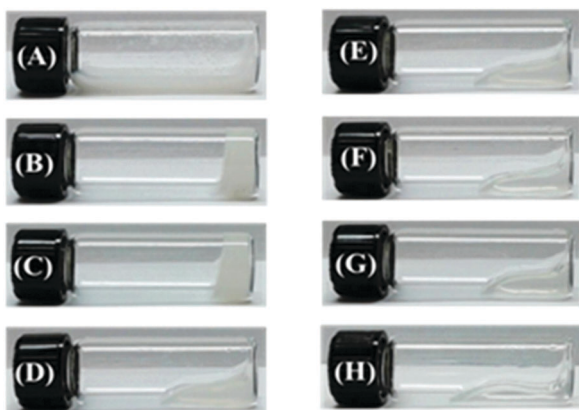


Fig. 2 Optical images of the Nap-FFC hydrogel ([Nap-FFC] = 1 wt%). The Nap-FFC hydrogel (1 wt%) exists as (A) a precipitates at pH < 4.0, (B and C) a strongly opaque hydrogel at a pH range of about 4.0 to 6.0, (D–G) a weak transparent hydrogel at a pH range of about 7.0 to 10.0, and (H) a clear solution at pH > 10.

completely soluble at pH > 10, due to the stable deprotonation of the compound under highly alkaline conditions. Interestingly, the Nap-FFC hydrogel (1% w/v) was semi-transparent at pH ranging from 7 to 10, but in the acidic pH range (5 to 6) the hydrogel was opaque. In addition, at low pH (pH = 4) the 1% (w/v) Nap-FFC hydrogel was starting to form a precipitate, which might be because of stable protonation. The formation of a hydrogel within a narrow pH range (5 to 6) likely arises from a balance of protonation/deprotonation of the C-terminal carboxyl group.^{25–27}

FT-IR analysis

The interaction of the Nap-FFC peptide with silver ions was studied using FT-IR analysis, as shown in Fig. S8 (ESI†). The IR peak indicates the presence of C=O groups at 1670 cm⁻¹ and the S–H stretching of Nap-FFC at 2569 cm⁻¹.²⁸ Interestingly, the S–H and C=O stretching bands at 2569, 1670 cm⁻¹ of Nap-FFC were absent due to the binding of silver ions to the carbonyl and thiol terminals of Nap-FFC. According to the above results, the Nap-FFC peptide displayed a carboxylic acid and thiol group on the supramolecule nanofiber surface, which offers the strong interaction with silver ions.^{29,30}

Stability of the AgNPs@Nap-FFC nanocomposite

To examine stability, the Nap-FFC peptide nanocomposites (AgNPs@Nap-FFC) produced *via* the *in situ* reduction method was compared with bare AgNPs (NaBH₄ reduced) using UV-vis absorption spectroscopy. The UV-vis absorption spectra of the bare AgNPs and AgNPs@Nap-FFC show a surface plasmon resonance (SPR) absorption peak at 400 nm and 420 nm, respectively, as shown in Fig. 3(A) and (B). The characteristic SPR peaks of the bare AgNPs at 400 nm showed large decrements in the absorption intensity within seven days due to the serious aggregation of AgNPs that usually leads to a significant decrease in the antibacterial effect. The SPR band of the AgNPs@Nap-FFC nanocomposites is somewhat longer than that of typical bare AgNPs and this red-shift in wavelength is due to the high dielectric constant of the Nap-FFC peptide, which lowers the plasmon frequency.^{31,32} On the other hand, the UV-vis spectra of the AgNPs@Nap-FFC nanocomposites showed only a slight change in the shifting of the SPR band (~2 nm) over a time period of 30 days. Thus, the AgNPs@Nap-FFC peptide nanocomposites

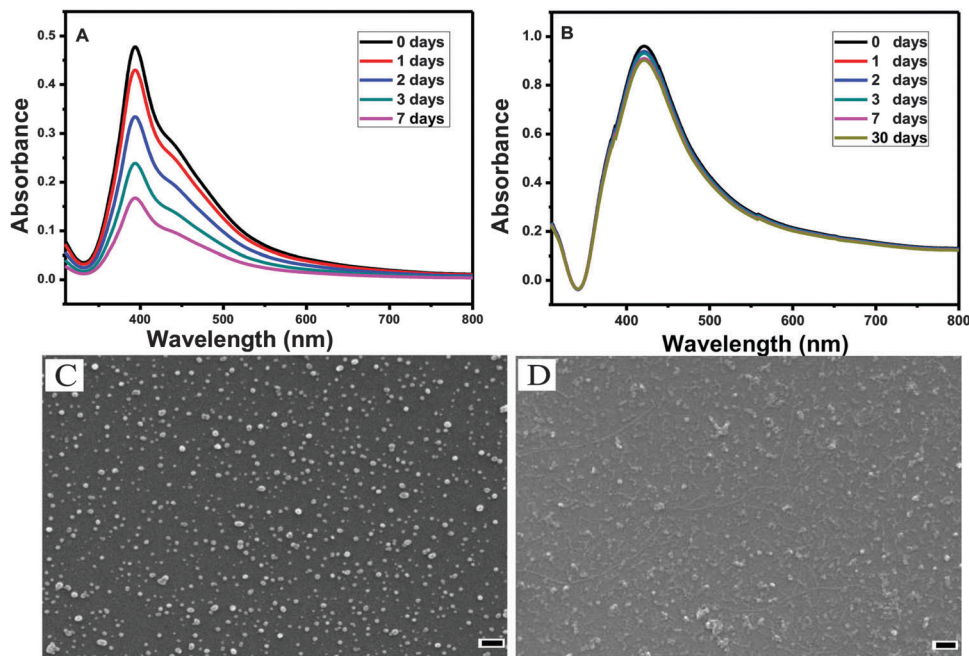


Fig. 3 The absorption spectra and SEM analysis of the AgNPs (A and C) and AgNPs@Nap-FFC nanocomposite (B and D) at pH 7.4. Scale bar: 100 nm.

specify long term high stability. Furthermore, the morphologies of the bare AgNPs and AgNPs@Nap-FFC peptide nanocomposites were examined *via* SEM analysis and the images are shown in Fig. 3(C) and (D), respectively. The average size of the bare AgNPs and mineralised AgNPs obtained from the Nap-FFC nanofibers are approximately ~ 15 nm and ~ 10 nm, respectively. TEM analysis further confirms the size of the AgNPs and AgNPs@Nap-FFC peptide nanocomposites (shown in Fig. S9, ESI[†]). Therefore, the newly developed AgNPs@Nap-FFC peptide nanocomposite has a high monodispersity and long term stability even in aqueous medium.

For antibacterial applications, the hydrogel was formed by combining $80 \mu\text{g mL}^{-1}$ AgNPs@Nap-FFC peptide nanocomposites (liquid form) with 1% Nap-FFC (no AgNPs present) at pH 12. Also, the effect of gelation of AgNPs@Nap-FFC was systematically studied at different periods (shown in Fig. S10, ESI[†]). According to the photographic images, the time dependent gelation can be seen when $80 \mu\text{g mL}^{-1}$ AgNPs@Nap-FFC was added to 1% Nap-FFC, which was able to form hydrogels overnight. No characteristic gelation was seen at 30 min even in the presence of AgNPs@Nap-FFC but hydrogel formation was observed after overnight incubation, due to the self-assembly process of Nap-FFC, with respect to time. On the contrary, we also observe that the clear solution of 1% Nap-FFC (w/v) without AgNPs@Nap-FFC does not change phase after an overnight time period. The SEM image (Fig. 4A and B), ensured the morphology of the 1% (w/v) Nap-FFC with/without AgNPs@Nap-FFC nanocomposites ($80 \mu\text{g mL}^{-1}$) and we noticed the uniform dispersion of AgNPs on the surface of the Nap-FFC nanofiber. Further confirmation of the presence of AgNPs in NapFFC nanocomposites was done *via* EDX analysis (Fig. 4C). The peak in the EDX spectra indicates the presence of silver at 3 keV and the C and O

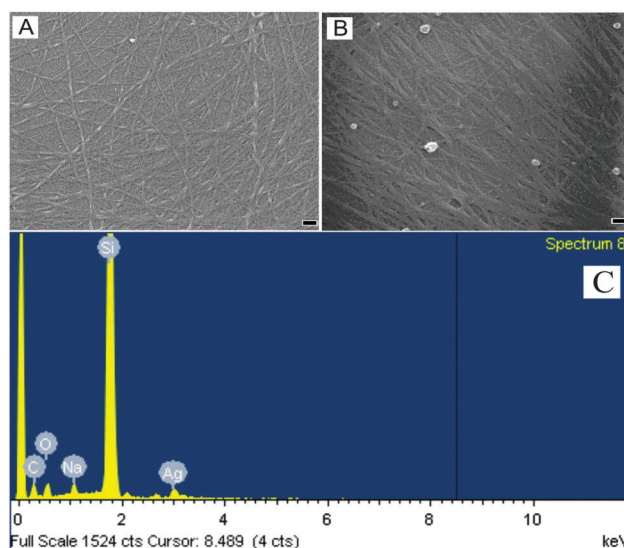


Fig. 4 The SEM analysis (A and B) of 1% (w/v) Nap-FFC without/with $80 \mu\text{g mL}^{-1}$ AgNPs@Nap-FFC. The EDX analysis (C) of 1% (w/v) Nap-FFC containing $80 \mu\text{g mL}^{-1}$ AgNPs@Nap-FFC. Scale bar: 100 nm.

peak at 0.2 and 0.4 keV, respectively, which is related to the amino acid of Nap-FFC.

Bacterial kinetic test

A bacterial kinetic test was performed to determine the antibacterial activity of the Nap-FFC and AgNPs@Nap-FFC nanocomposites. As shown in Fig. 5, a comparison of the growth curves of the control bacteria to the test bacteria shows that Nap-FFC at $120 \mu\text{M}$ did not alter the growths of *S. aureus* and

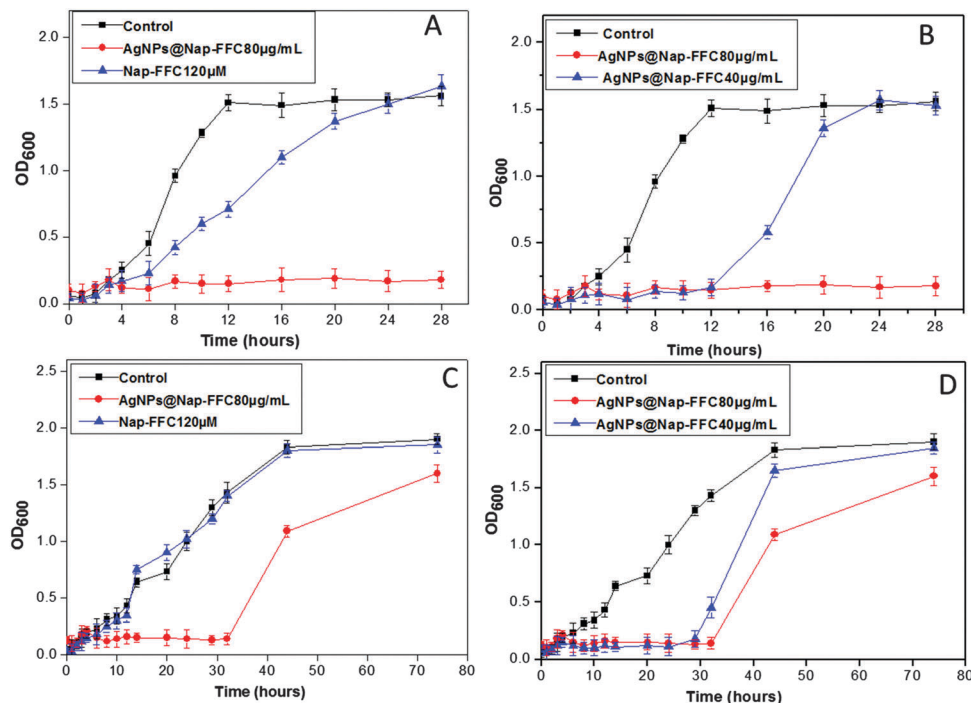


Fig. 5 Bacterial growth curves in Luria-Bertani (LB) media with Nap-FFC or AgNPs@Nap-FFC nanocomposites stored at 4 °C for 7 days. Comparison of the antibacterial activity of Nap-FFC and AgNPs@Nap-FFC against methicillin-resistant *Staphylococcus aureus* (A and B) and *Acinetobacter baumannii* (C and D).

A. baumannii, suggesting that it has no inhibitory effect on these bacteria (Fig. 5A and C). On the other hand, even $40 \mu\text{g mL}^{-1}$ of AgNPs@Nap-FFC was able to slow down the growth of both *S. aureus* and *A. baumannii* at 12 and 28 h, respectively. Moreover, when the concentration of AgNPs@Nap-FFC was increased to $80 \mu\text{g mL}^{-1}$ (Fig. 5B and D), the growth of both bacteria showed strong long-term inhibition, revealing that these nanocomposites can be an attractive biomaterial for applications such as wound dressing.

Bacterial spread plate method

The antibacterial activity of the Nap-FFC and AgNPs@Nap-FFC nanocomposites were further ensured *via* the bacterial spread plate method. For this, Nap-FFC without/with AgNPs@Nap-FFC was layered over a lawn of *S. aureus* and *A. baumannii* in a TSA plate, and incubated at room temperature for 12 and 24 hours. After 12 hours of incubation, only AgNPs@Nap-FFC ($80 \mu\text{g mL}^{-1}$) produced a clearly visible area of inhibition (Fig. 6 and 7), suggesting an excellent bacterial inhibition property due to the release of a large amount of nanosilver particles (Fig. 6 and 7). The antibacterial activity was maximal and then decreased after 24 hours of incubation due to a gradual decrease in the amount of nanosilver particles released, which was also reported in previous studies.³³ Henceforth, the resumed growth of both bacteria occurred when the concentration of nanosilver decreased below the minimum inhibitory concentration. So we speculate that under different time phases, the decreasing nanosilver concentration may result in lower antibacterial activity.

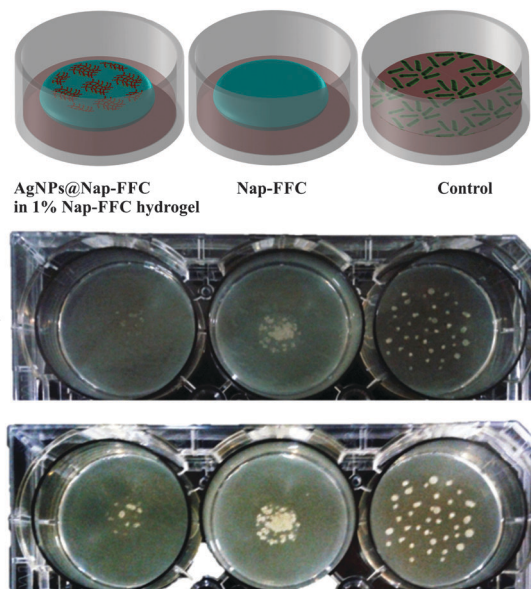


Fig. 6 Schematic illustration of the antibacterial test of the Nap-FFC and AgNPs@Nap-FFC hydrogels; Petri plates with Luria-Bertani (LB)-agar inoculated with methicillin-resistant *Staphylococcus aureus*, showing variable numbers of colonies when supplemented with 1% (w/v) Nap-FFC with/without $80 \mu\text{g mL}^{-1}$ AgNPs@Nap-FFC.

Biocompatibility of the AgNPs@Nap-FFC nanocomposites

To further test the potential applications of the AgNPs@Nap-FFC nanocomposites, we evaluated the toxic effects of these nanocomposites in human HeLa cells using an MTT assay.

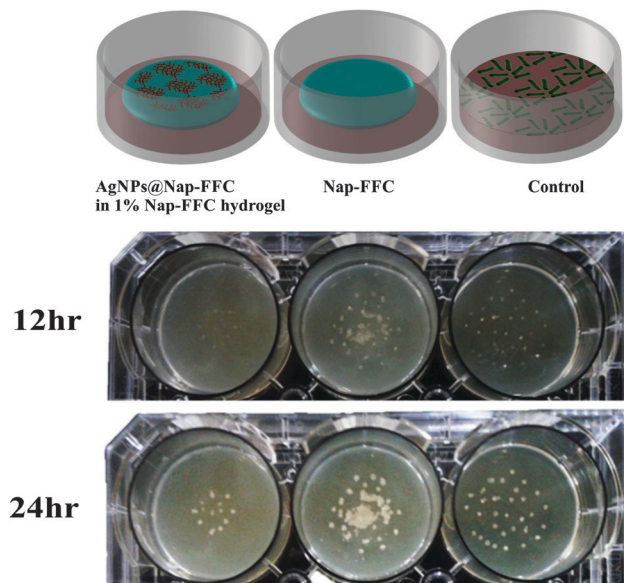


Fig. 7 Schematic illustration of the antibacterial test of Nap-FFC and AgNPs@Nap-FFC hydrogels; Petri plates with Luria-Bertani (LB)-agar inoculated with *Acinetobacter baumannii*, showing variable numbers of colonies when supplemented with 1% (w/v) Nap-FFC with/without $80 \mu\text{g mL}^{-1}$ AgNPs@Nap-FFC.

After 24 hours of incubation, we found that the AgNPs@Nap-FFC nanocomposites showed no or little effect on HeLa cells at concentrations up to $80 \mu\text{g mL}^{-1}$ (Fig. 8). Even after increasing the concentration of the AgNPs@Nap-FFC nanocomposite up to $100 \mu\text{g mL}^{-1}$, they displayed only a mild decrease in human cell viability ensuring its lower cytotoxicity and proving to reduce the risk of harmful side effects. Moreover, the Nap moiety adopted to prepare this peptide has been used in clinically approved drug molecules such as propranolol and naphazoline,²³ which adds more safety to this nanocomposites. The supramolecular

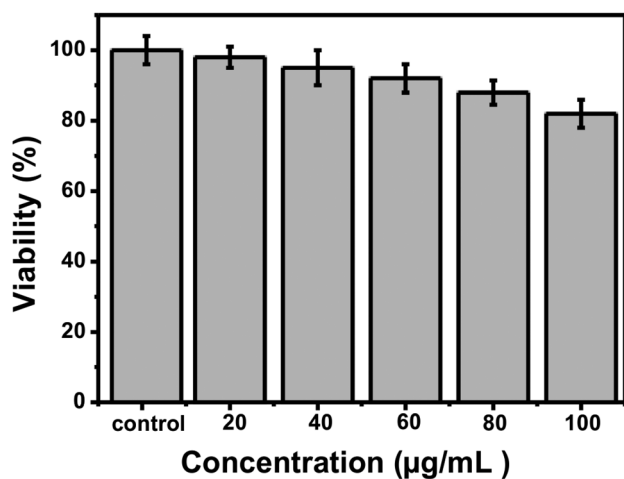


Fig. 8 Cytotoxicity assay of the AgNPs@Nap-FFC nanocomposites at pH 7.4. The viability of HeLa cells incubated with different concentrations ($20, 40, 60, 80, 100 \mu\text{g mL}^{-1}$) of the AgNPs@Nap-FFC nanocomposites for 24 h. Each data point represents the mean values from at least three independent experiments.

hydrogel can provide the moisture environment to enhance human cell growth. Overall, 80–90% of the cells were found to be viable at 40 and $80 \mu\text{g mL}^{-1}$ concentrations of the AgNPs@Nap-FFC nanocomposites. These data suggested that the AgNPs@Nap-FFC nanocomposite has a favourable biocompatibility towards human cells.

Conclusions

In summary, we report the synthesis of Nap-FFC peptide based nanofibers which were utilized to produce AgNPs@Nap-FFC nanocomposites *via* a mineralization process. After the successful synthesis, Nap-FFC and AgNPs@Nap-FFC were characterized *via* NMR, high resolution mass analysis, SEM, TEM, FTIR and EDX. This silver based nanocomposite (AgNPs@Nap-FFC) offered an extended stability of approximately 30 days compared to that of bare AgNPs (NaBH_4 reduced). Also, the factors which influence the formation of hydrogels such as the effect of gelation at different pH values and mineralization of the Nap-FFC peptide with various metal ions were systematically studied. The results revealed that the interaction of the Nap-FFC peptides with Ag^+ ions was more pronounced due to the presence of carboxyl and thiol groups in Nap-FFC, resulting in the formation of AgNPs@Nap-FFC. The optimum conditions to prepare AgNPs@Nap-FFC are 1% Nap-FFC (w/v) at pH 12 at 30°C . For the antibacterial study, a hydrogel pad was prepared by mixing AgNPs@Nap-FFC ($80 \mu\text{g mL}^{-1}$) in 1% Nap-FFC (w/v) peptide. These nanocomposite pads showed a strong antibacterial effect against both Gram-positive and Gram-negative bacteria. Moreover, the nanocomposites displayed significant biocompatibility towards HeLa cells. Therefore, the prepared AgNPs@Nap-FFC peptide nanocomposites are promising candidates for antibacterial soft materials for future tissue engineering and wound dressing.

Acknowledgements

The authors are grateful to the National Taiwan University Hospital Hsinchu Branch and the Ministry of Science and Technology of Taiwan for financially supporting this research under the contract MOST 101-2113-M-009-007-MY3.

References

- (a) S. Ningangouda, V. Rathod, D. Singh, J. Hiremath, A. K. Singh, J. Mathew and M. ul-Haq, *BioMed Res. Int.*, 2014, **2014**, 9; (b) L. Liu, J. Liu, Y. Wang, X. Yan and D. D. Sun, *New J. Chem.*, 2011, **35**, 1418.
- Y. Wang, L. Cao, S. Guan, G. Shi, Q. Luo, L. Miao, I. Thistlethwaite, Z. Huang, J. Xu and J. Liu, *J. Mater. Chem.*, 2012, **22**, 2575.
- (a) S. Agnihotri, G. Bajaj, S. Mukherji and S. Mukherji, *Nanoscale*, 2015, **7**, 7415; (b) S. Agnihotri, S. Mukherji and S. Mukherji, *RSC Adv.*, 2014, **4**, 3974.
- (a) Y. Zhou, M. Kogiso, M. Asakawa, S. Dong, R. Kiyama and T. Shimizu, *Adv. Mater.*, 2009, **21**, 1742; (b) S. Pal, Y. K. Tak,

- E. Han, S. Rangasamy and J. M. Song, *New J. Chem.*, 2014, **38**, 3889.
- 5 (a) S. Gurunathan, J. W. Han, D. N. Kwon and J. H. Kim, *Nanoscale Res. Lett.*, 2014, **9**, 373; (b) A. Chowdhuri, S. Tripathy, C. Haldar, B. Das, S. Roy and S. K. Sahu, *RSC Adv.*, 2015, **5**, 21515.
- 6 (a) S. Chernousova and M. Epple, *Angew. Chem., Int. Ed.*, 2013, **52**, 1636; (b) L. Shahriary, R. Nair, S. Sabharwal and A. A. Athawale, *New J. Chem.*, 2015, **39**, 4583.
- 7 A. Shome, S. Duta, S. Maiti and P. K. Das, *Soft Matter*, 2011, **7**, 3011.
- 8 M. Lv, S. Su, Y. He, Q. Huang, W. Hu, D. Li, C. Fan and S. T. Lee, *Adv. Mater.*, 2010, **22**, 5463.
- 9 M. Auffan, J. Rose, M. R. Wiesner and J. Y. Bottero, *Environ. Pollut.*, 2009, **157**, 1127.
- 10 Y. Cheng, L. Yin, S. Lin, M. Wiesner, E. Bernhardt and J. Liu, *J. Phys. Chem. C*, 2011, **115**, 4425.
- 11 (a) J. Jain, S. Arora, J. M. Rajwade, P. Omray, S. Khandelwal and K. M. Paknikar, *Mol. Pharmaceutics*, 2009, **6**, 1388; (b) Z. Mao, X. Zhou and C. Gao, *Biomater. Sci.*, 2013, **1**, 896.
- 12 (a) J. J. Lin, W. C. Lin, R. X. Dong and S. H. Hsu, *Nanotechnology*, 2012, **23**, 065102; (b) T. Maneerunga, S. Tokurab and R. Rujiravanit, *Carbohydr. Polym.*, 2008, **72**, 43; (c) V. R. Babu, C. Kim, S. Kim, C. Ahn and Y. I. Lee, *Carbohydr. Polym.*, 2010, **81**, 196.
- 13 T. T. H. Anh, M. Xing, D. H. T. Le, A. Sugawara-Narutaki and E. Fong, *Nanomedicine*, 2013, **8**, 567.
- 14 (a) J.M. Galloway and S. S. Staniland, *J. Mater. Chem.*, 2012, **22**, 12423; (b) Y. Li, F. Zho, Y. Wen, K. Liu, L. Chen, Y. Mao, S. Yang and T. Yi, *Soft Matter*, 2014, **10**, 3077; (c) A. Shockravi, A. Jawadi and E. A. Lotf, *RSC Adv.*, 2013, **3**, 6717.
- 15 M. J. Webber, J. Tongers, M. A. Renault, J. G. Roncalli, D. W. Losordo and S. I. Stupp, *Acta Biomater.*, 2010, **6**, 3.
- 16 G. A. Silva, C. Czeisler, K. L. Niece, E. Beniash, D. A. Harrington and J. A. Kessler, *Science*, 2004, **303**, 1352.
- 17 (a) J. B. Matson, R. H. Zha and S. I. Stupp, *Curr. Opin. Solid State Mater. Sci.*, 2011, **15**, 225; (b) C. HeLary, A. Abed, G. Mosser, L. Louedec, D. Letourneur, T. Coradin, M. M. G. Guillea and A. M. Pelle, *Biomater. Sci.*, 2015, **3**, 373.
- 18 E. D. Spoerke, S. G. Anthony and S. I. Stupp, *Adv. Mater.*, 2009, **21**, 425.
- 19 (a) X. Zhao, F. Pan and J. R. Lu, *Prog. Nat. Sci.*, 2008, **18**, 653; (b) M. Malmsten, *Soft Matter*, 2011, **7**, 8725.
- 20 X. Yan, P. Zhu and J. Li, *Chem. Soc. Rev.*, 2010, **39**, 1877.
- 21 Y. Pan, Y. Gao, J. Shi, L. Wang and B. Xu, *J. Mater. Chem.*, 2011, **21**, 6804.
- 22 M. Zhang and B. C. Ye, *Anal. Chem.*, 2011, **83**, 1504.
- 23 Z. Yang and B. Xu, *J. Mater. Chem.*, 2007, **17**, 2385.
- 24 Z. Luo and S. Zhang, *Chem. Soc. Rev.*, 2012, **41**, 4736.
- 25 Y. Kuang, Y. Gao and B. Xu, *Chem. Commun.*, 2011, **47**, 12625.
- 26 X. Yan, F. Wang, B. Zheng and F. Huang, *Chem. Soc. Rev.*, 2012, **41**, 6042.
- 27 J. F. Miravet and B. Escuder, *Chem. Commun.*, 2005, 5796.
- 28 E. Cevher, D. Sensoy, M. A. M. Taha and A. Araman, *AAPS PharmSciTech*, 2008, **9**, 953.
- 29 S. K. Tripathy and Y. T. Yu, *Spectrochim. Acta, Part A*, 2009, **72**, 841.
- 30 A. Ravindran, N. Chandrasekaran and A. Mukherjee, *Curr. Nanosci.*, 2012, **8**, 141.
- 31 A. Shome, S. Dutta, S. Maiti and P. K. Das, *Soft Matter*, 2011, **7**, 3011.
- 32 X. Li, J. Zhang, W. Xu, H. Jia, X. Wang, B. Yang, B. Zhao, B. Li and Y. Ozaki, *Langmuir*, 2003, **19**, 4285.
- 33 (a) Z. M. Xiu, Q. B. Zhang, H. L. Puppala, V. L. Colvin and P. J. J. Alvarez, *Nano Lett.*, 2012, **12**, 4271; (b) Y. Zhou, Y. Zhao, L. Wang, L. Xu, M. Zhai and S. Wei, *Radiat. Phys. Chem.*, 2012, **81**, 553.